J. Fluid Mech. (2004), *vol.* 500, *pp.* 103–112.
DOI: 10.1017/S0022112003007341 Printed in the United Kingdom

Three-dimensional stability of a Burgers vortex

By PETER J. SCHMID† AND MAURICE ROSSI

Laboratoire de Modélisation en Mécanique (LMM), Université Paris VI, 4 place Jussieu, F-75252 Paris, Cedex 05, France

(Received 14 August 2003 and in revised form 5 November 2003)

The evolution of infinitesimal three-dimensional perturbations superimposed on a Burgers vortex is studied. By a sequence of variable transformations and scalings this linear evolution problem is reduced to a time-dependent system which is nearly identical to the stability equations governing a Lamb–Oseen vortex. The maximum amplification reached by perturbations over a finite time interval is computed through an iterative scheme based on the direct and adjoint governing equations, and results on the asymptotic stability of the Burgers vortex are deduced. The Burgers vortex is shown to be asymptotically stable, although significant short-term amplification may occur.

1. Introduction

Numerical simulations (Vincent & Meneguzzi 1991; Jimenez *et al.* 1993) and experiments (Cadot, Douady & Couder 1995) on turbulent flows have produced abundant evidence of the importance of the vortex stretching mechanism. In particular, the balance between vorticity production by stretching (Saffman 1992) and vortex diffusion has been studied extensively since it is believed to represent the underlying dynamic mechanism for vortex-dominated flows. It thus should not be surprising that the uniformly stretched vortex, the so-called Burgers vortex (Lundgren 1982; see also Pullin & Saffman 1998), as well as its asymmetric companion (Moffatt, Kida & Ohkitani 1994) have repeatedly been used to model generic vortex filament behaviour in high-resolution numerical simulations. These models have, however, been of limited value since the alignment of the vorticity vector with the vortex axis and with a principal direction of strain has rendered them of somewhat limited physical significance.

Various extensions of the basic models to more complex situations have been proposed (Rossi 2000). Radial dependence of the strain rate, but independence of the axial velocity of the axial coordinate direction has been considered by Gibbon, Fokas & Doering (1999), while Le Dizès, Rossi & Moffatt (1996) and Eloy & Le Dizès (1999) studied ways to suppress the elliptic instability by axial stretching. Verzicco, Jiménez & Orlandi (1995) addressed the effect of local compression on the vortex dynamics.

General results on the stability of the Burgers vortex are rather limited. Purely two-dimensional perturbations have been studied by Robinson & Saffman (1984) where an analytical solution for low Reynolds numbers has been obtained. These results have subsequently been extended by Prochazka & Pullin (1995) for Reynolds numbers

† Permanent address: Department of Applied Mathematics, University of Washington, Seattle, WA 98195-2420, USA.

up to $Re = 10^4$. Both studies concluded that the temporal spectrum associated with two-dimensional perturbations is discrete and contains only damped modes. Rossi & Le Dizès (1997) showed that the discrete part of the temporal spectrum of steady stretched vortices contains only modes which do not depend on the axial coordinate (stretching axis), i.e. are purely two-dimensional. The *global monotonic* stability of the Burgers vortex has been addressed by Leibovitch & Holmes (1981) who showed that no finite critical viscosity exists for such a problem. Recently, Crowdy (1998) derived analytical dispersion relations for the evolution of axisymmetric disturbances in the asymptotic limit of large axial distances and small Reynolds numbers. To our knowledge, a general study of the linear evolution of three-dimensional perturbations on an axisymmetric Burgers vortex has not been attempted thus far. An analysis of this problem is the main focus of this article.

2. Linearized equations for three-dimensional perturbations

The well-known Burgers vortex describes an axisymmetric vortex subjected to an axial strain field of constant strain rate γ. The velocity field (U^{Burg}, V^{Burg}, W^{Burg}) is expressed in polar coordinates (r, θ, z) as

$$U^{\mathrm{Burg}} = -\tfrac{1}{2}\gamma r, \quad W^{\mathrm{Burg}} = \gamma z, \tag{2.1a}$$

$$V^{\mathrm{Burg}} = \frac{\Gamma}{2\pi r}\left(1 - \exp\left(-\frac{r^2}{a_0^2}\right)\right), \tag{2.1b}$$

with $a_0^2 = 4\nu/\gamma$. This steady velocity field represents one of the few three-dimensional exact solutions of the Navier–Stokes equations: the azimuthal velocity component is characterized by the circulation Γ, and the stretching field counteracts the diffusion of the vortex core due to the kinematic viscosity ν. We recall that this base flow can be related to an unstretched vortex solution. This is accomplished using the elegant Lundgren transformation (Lundgren 1982)

$$r \longrightarrow \bar{r} = \sqrt{s(t)}r, \quad \theta \longrightarrow \theta, \tag{2.2a}$$

$$t \longrightarrow \bar{t} = \int_0^t s(u)\ \mathrm{d}u = \frac{1}{\gamma}(\exp(\gamma t) - 1), \tag{2.2b}$$

with $s(t) \equiv \exp(\gamma t)$. Using these generalized space and time coordinates, the Burgers vortex (2.1) can be recast as a diffusing Lamb–Oseen vortex $(0, \bar{V}^{2\mathrm{D}}(\bar{r}, \bar{t}), 0)$ with

$$\bar{V}^{2D}(\bar{r}, \bar{t}) = \frac{V^{\mathrm{Burg}}(\bar{r}/\sqrt{s(t)})}{\sqrt{s(t)}} = \frac{\Gamma}{2\pi\bar{r}}\left(1 - \exp\left(-\frac{\bar{r}^2}{a^2(\bar{t})}\right)\right), \tag{2.3}$$

where the vortex core size $a(\bar{t})$ increases due to viscous diffusion, namely $a^2(\bar{t}) = a_0^2 + 4\nu\bar{t}$ with a_0 denoting the initial core size.

We proceed by analysing the evolution of infinitesimal three-dimensional perturbations superimposed on the Burgers vortex $\boldsymbol{U}^{\mathrm{Burg}}(r, z)$. The governing equations are

$$\frac{\partial \boldsymbol{u}}{\partial t} + (\boldsymbol{U}^{\mathrm{Burg}}(r, z)\cdot\nabla)\boldsymbol{u} + (\boldsymbol{u}\cdot\nabla)\boldsymbol{U}^{\mathrm{Burg}}(r, z) = -\nabla p + \nu\Delta\boldsymbol{u}, \quad \nabla\cdot\boldsymbol{u} = 0, \tag{2.4}$$

where $\boldsymbol{u}$ and p denote the disturbance velocity and pressure, respectively. Owing to the explicit z-dependence in (2.1) standard Fourier transform techniques fail to provide an efficient method of treating the resulting stability problem. In what follows we outline a sequence of manipulations that transforms equations (2.4) into a set of

linear equations which are nearly identical to the equations governing the dynamics of infinitesimal perturbations on an axisymmetric unstretched time-dependent vortex, i.e. the diffusing Lamb–Oseen vortex.

We apply Lundgren's transformation (2.2) to the three-dimensional perturbation equations (2.4) together with the following set of mappings for the independent z-variable as well as for the pressure (p) and for the radial (u), azimuthal (v), and axial (w) velocities:

$$z \longrightarrow \bar{z} = \frac{z}{S}, \quad \bar{p} = \frac{p}{S}, \quad \bar{u} = \frac{u}{\sqrt{S}}, \quad \bar{v} = \frac{v}{\sqrt{S}}, \quad \bar{w} = Sw, \tag{2.5}$$

where we have introduced the non-dimensional quantity $S(\bar{t}) \equiv s(t) = 1 + \gamma\bar{t}$ (see (2.2*b*)). The transformation of the independent variable z in (2.5) can equivalently be expressed in terms of a time-dependent axial wavenumber – a technique commonly used in the context of inertial waves (see Craik & Criminale 1986) or rapid distortion theory (Batchelor & Proudman 1954; Cambon & Scott 1999). In addition, the scalings of the quantities u, v, w, p are designed to balance the amplifying effects of stretching. It is important to note that neither the partial derivatives with respect to the azimuthal coordinate θ nor the elementary infinitesimal volume $r\,\mathrm{d}r\,\mathrm{d}\theta\,\mathrm{d}z$ are affected by the sequence of transformations (2.2) and (2.5). Due to these changes, the terms in (2.4) related to stretching – such as $-\frac{1}{2}\gamma r(\partial \boldsymbol{u}/\partial r)$, $\gamma z(\partial \boldsymbol{u}/\partial z)$, $-\frac{1}{2}\gamma u$, γw – are eliminated, and stretching effects are accounted for by the time-dependent term $S(\bar{t})$. For instance, the convective derivative is

$$\frac{\mathrm{D}}{\mathrm{D}t} = S(\bar{t})\frac{\bar{\mathrm{D}}}{\bar{\mathrm{D}}\bar{t}} \quad \text{with} \quad \frac{\bar{\mathrm{D}}}{\bar{\mathrm{D}}\bar{t}} \equiv \frac{\partial}{\partial \bar{t}} + \frac{\bar{V}^{2\mathrm{D}}(\bar{r},\bar{t})}{\bar{r}}\frac{\partial}{\partial\theta}. \tag{2.6}$$

The complete linear system, after applying the above transformations, is then

$$\frac{\bar{\mathrm{D}}\bar{u}}{\bar{\mathrm{D}}\bar{t}} - 2\frac{\bar{V}^{2\mathrm{D}}}{\bar{r}}\bar{v} = -\frac{\partial\bar{p}}{\partial\bar{r}} + \nu\left[(\Delta^{2D}\bar{\boldsymbol{u}})_{\bar{r}} + \frac{1}{S^3}\frac{\partial^2\bar{u}}{\partial\bar{z}^2}\right], \tag{2.7a}$$

$$\frac{\bar{\mathrm{D}}\bar{v}}{\bar{\mathrm{D}}\bar{t}} + \left(\frac{\partial\bar{V}^{2\mathrm{D}}}{\partial\bar{r}} + \frac{\bar{V}^{2\mathrm{D}}}{\bar{r}}\right)\bar{u} = -\frac{1}{\bar{r}}\frac{\partial\bar{p}}{\partial\theta} + \nu\left[(\Delta^{2D}\bar{\boldsymbol{u}})_{\theta} + \frac{1}{S^3}\frac{\partial^2\bar{v}}{\partial\bar{z}^2}\right], \tag{2.7b}$$

$$\frac{\bar{\mathrm{D}}\bar{w}}{\bar{\mathrm{D}}\bar{t}} = -\frac{\partial\bar{p}}{\partial\bar{z}} + \nu\left[(\Delta^{2D}\bar{\boldsymbol{u}})_{\bar{z}} + \frac{1}{S^3}\frac{\partial^2\bar{w}}{\partial\bar{z}^2}\right], \tag{2.7c}$$

$$\frac{\partial\bar{u}}{\partial\bar{r}} + \frac{\bar{u}}{\bar{r}} + \frac{1}{\bar{r}}\frac{\partial\bar{v}}{\partial\theta} + \frac{1}{S^3}\frac{\partial\bar{w}}{\partial\bar{z}} = 0, \tag{2.7d}$$

where $\Delta^{2D}\bar{\boldsymbol{u}}$ denotes the vector Laplacian operator in the cross-sectional $(\bar{r},\theta)$-plane

$$(\Delta^{2D}\bar{\boldsymbol{u}})_{\bar{r}} = \frac{\partial}{\partial\bar{r}}\left(\frac{1}{\bar{r}}\frac{\partial}{\partial\bar{r}}(\bar{r}\bar{u})\right) + \frac{1}{\bar{r}^2}\frac{\partial^2\bar{u}}{\partial\theta^2} + \frac{2}{\bar{r}^2}\frac{\partial\bar{v}}{\partial\theta},$$

$$(\Delta^{2D}\bar{\boldsymbol{u}})_{\theta} = \frac{\partial}{\partial\bar{r}}\left(\frac{1}{\bar{r}}\frac{\partial}{\partial\bar{r}}(\bar{r}\bar{v})\right) + \frac{1}{\bar{r}^2}\frac{\partial^2\bar{v}}{\partial\theta^2} - \frac{2}{\bar{r}^2}\frac{\partial\bar{u}}{\partial\theta},$$

$$(\Delta^{2D}\bar{\boldsymbol{u}})_{\bar{z}} = \frac{1}{\bar{r}}\frac{\partial}{\partial\bar{r}}\left(\bar{r}\frac{\partial\bar{w}}{\partial\bar{r}}\right) + \frac{1}{\bar{r}^2}\frac{\partial^2\bar{w}}{\partial\theta^2}.$$

The transformed system (2.7) is autonomous in the axial variables and is thus amenable to Fourier transforms in the axial direction. Moreover, the above manipulation illustrates that the stability of a stretched Burgers vortex with respect to two-dimensional ($\partial/\partial\bar{z} \equiv 0$) perturbations is equivalent to the stability of an

equivalent unstretched but diffusing Lamb–Oseen vortex $(0, \hat{V}^{2D}(\bar{r}, \bar{t}), 0)$. For general three-dimensional perturbations, the difference between the equations for the stretched Burgers vortex and the equations for the diffusing Lamb–Oseen vortex consists merely of the appearance of the time-dependent $1/S^3$ terms associated with derivatives with respect to $\bar{z}$. These time-dependent terms appear in the conservation equations for both momentum and mass.

In the subsequent analysis, the time origin is shifted by $1/\gamma$ so that the time origin corresponds to the instant when the Lamb–Oseen vortex is singular:

$$\bar{t}^* \equiv \bar{t} + \frac{1}{\gamma} \quad \text{so that} \quad S(\bar{t}^*) = \gamma \bar{t}^*, \quad a^2(\bar{t}^*) = 4\nu \bar{t}^*, \quad \ln\left(\frac{\bar{t}^*}{\bar{t}_1^*}\right) = \gamma t \quad \text{with} \quad \bar{t}_1^* \equiv 1/\gamma, \tag{2.8}$$

where (2.2*b*) has been used. From now on, the asterisk superscript in time $\bar{t}^*$ is omitted. A disturbance thus evolves over a time period $[\bar{t}_1, \infty[$. This interval is subsequently divided into a sequence of disjoint subintervals $[\bar{t}_p, \bar{t}_{p+1}]$ where $\bar{t}_p \equiv \alpha^{p-1}\bar{t}_1$ and α is an arbitrary constant strictly greater than one. Definition (2.8) shows that, at time $\bar{t}_p$, the vortex core size $a(\bar{t})$ is equal to $2\delta_p$ with $\delta_p = (\nu \bar{t}_p)^{1/2}$. Within each subinterval $[\bar{t}_p, \bar{t}_{p+1}]$ we proceed by non-dimensionalizing the governing equations (2.7) by appropriately chosen scales: the radial $(\bar{u})$ and azimuthal $(\bar{v})$ velocity components are non-dimensionalized by Γ/δ_p, the axial velocity component $\bar{w}$ by $(\Gamma/\delta_p)(\gamma \bar{t}_p)^{3/2}$, and the pressure p by $(\Gamma/\delta_p)^2$. The independent variables $\bar{t}, \bar{r}$, and $\bar{z}$ are non-dimensionalized by $\bar{t}_p, \delta_p$, and $\delta_p(\gamma \bar{t}_p)^{-3/2}$, respectively. In what follows, superscripts $\hat{}$(resp.$^-$) denote non-dimensional (resp. dimensional) quantities or space/time variables in the transformed space. When these superscripts are absent, quantities or space/time variables are assumed to be dimensional and written in physical space. Within each subinterval, the non-dimensional linear problem is

$$\frac{\hat{\mathrm{D}}\hat{u}}{\hat{\mathrm{D}}\hat{t}} - 2\frac{\hat{V}^{2D}}{\hat{r}}\hat{v} = -\frac{\partial \hat{p}}{\partial \hat{r}} + \frac{1}{Re_\Gamma}\left[(\Delta^{2D}\hat{\boldsymbol{u}})_{\hat{r}} + \frac{1}{\hat{t}^3}\frac{\partial^2 \hat{u}}{\partial \hat{z}^2}\right], \tag{2.9a}$$

$$\frac{\hat{\mathrm{D}}\hat{v}}{\hat{\mathrm{D}}\hat{t}} + \left(\frac{\partial \hat{V}^{2D}}{\partial \hat{r}} + \frac{\hat{V}^{2D}}{\hat{r}}\right)\hat{u} = -\frac{1}{\hat{r}}\frac{\partial \hat{p}}{\partial \theta} + \frac{1}{Re_\Gamma}\left[(\Delta^{2D}\hat{\boldsymbol{u}})_\theta + \frac{1}{\hat{t}^3}\frac{\partial^2 \hat{v}}{\partial \hat{z}^2}\right], \tag{2.9b}$$

$$\frac{\hat{\mathrm{D}}\hat{w}}{\hat{\mathrm{D}}\hat{t}} = -\frac{\partial \hat{p}}{\partial \hat{z}} + \frac{1}{Re_\Gamma}\left[(\Delta^{2D}\hat{\boldsymbol{u}})_{\hat{z}} + \frac{1}{\hat{t}^3}\frac{\partial^2 \hat{w}}{\partial \hat{z}^2}\right], \tag{2.9c}$$

$$\frac{\partial \hat{u}}{\partial \hat{r}} + \frac{\hat{u}}{\hat{r}} + \frac{1}{\hat{r}}\frac{\partial \hat{v}}{\partial \theta} + \frac{1}{\hat{t}^3}\frac{\partial \hat{w}}{\partial \hat{z}} = 0 \tag{2.9d}$$

$$\frac{\hat{\mathrm{D}}}{\hat{\mathrm{D}}\hat{t}} \equiv \frac{1}{Re_\Gamma}\frac{\partial}{\partial \hat{t}} + \frac{\hat{V}^{2D}(\hat{r}, \hat{t})}{\hat{r}}\frac{\partial}{\partial \theta}, \tag{2.9e}$$

where the Reynolds numbers is defined as $Re_\Gamma = \Gamma/\nu$, and

$$\hat{V}^{2D}(\hat{r}, \hat{t}) = \frac{1}{2\pi \hat{r}}\left(1 - \exp\left(-\frac{\hat{r}^2}{4\hat{t}}\right)\right). \tag{2.10}$$

Note that equations (2.9) are independent of the interval $[\bar{t}_p, \bar{t}_{p+1}]$, and thus can be solved over the same non-dimensional interval $\hat{t} \in [1, \alpha]$. The evolution of three-dimensional disturbances on a Burgers vortex have thus been reduced to the study of the simplified equations (2.9) to be solved over a single finite time period. The full temporal dynamics of the three-dimensional perturbations can be recovered by

inverting the scalings and transformations (which depend on the sub-interval under consideration) that lead to (2.9).

The kinetic energy of perturbations superimposed on the Burgers vortex,

$$I(t) = \int (u^2(t) + v^2(t) + w^2(t)) r \, \mathrm{d}r \, \mathrm{d}\theta \, \mathrm{d}z, \tag{2.11}$$

is a natural and common measure of disturbance size. In (2.11), the integration is performed over the entire (r, θ, z) space and the perturbations are assumed to be compact within the integration domain. Transformations (2.2) and (2.5) are applied to relate expression (2.11) to an equivalent formula involving the solution of equations (2.7). We obtain

$$I(t) \equiv J(\bar{t}) = \int \left(S(\bar{t}) \bar{u}^2(\bar{t}) + S(\bar{t}) \bar{v}^2(\bar{t}) + \frac{1}{S^2(\bar{t})} \bar{w}^2(\bar{t}) \right) \bar{r} \, \mathrm{d}\bar{r} \, \mathrm{d}\theta \, \mathrm{d}\bar{z}. \tag{2.12}$$

Equations (2.7) can be Fourier transformed in the axial and azimuthal coordinate directions which introduces an axial wavenumber $\bar{k}$ and an azimuthal wavenumber m. We note that the constant axial wavenumber $\bar{k}$ corresponds to a temporally evolving wavenumber $k(t) = \bar{k}/s(t)$ in physical space. Since wavenumber pairs $(\bar{k}, m)$ evolve independently from each other and the energy (2.12) can be orthogonally decomposed in such a Fourier basis, we consider the individual contributions of each wavenumber pair $(\bar{k}, m)$

$$J(\bar{t}; \bar{k}, m) = \int_0^\infty \left(S(\bar{t}) \bar{u}(\bar{t}) \bar{u}^+(\bar{t}) + S(\bar{t}) \bar{v}(\bar{t}) \bar{v}^+(\bar{t}) + \frac{1}{S^2(\bar{t})} \bar{w}(\bar{t}) \bar{w}(\bar{t})^+ \right) \bar{r} \, \mathrm{d}\bar{r}, \tag{2.13}$$

where the superscript $^+$ denotes the complex conjugation. In what follows the dependence of J on the wavenumber pair $(\bar{k}, m)$ is omitted but implicitly assumed and only the cases $0 \leqslant m, 0 \leqslant k$ are considered. This does not pose a loss of generality since the linear problem (2.7) possesses the following symmetries: if $(\bar{u}(\bar{r}, \bar{t}), \bar{v}(\bar{r}, \bar{t}), \bar{w}(\bar{r}, \bar{t}))$ is a solution of (2.7) for the wavenumber pair $(\bar{k}, m)$, it is also a solution for the wavenumber pair $(-\bar{k}, m)$, and $(\bar{u}^+, \bar{v}^+, \bar{w}^+)$ is a solution for the wavenumber pair $(-\bar{k}, -m)$. Let us now consider an initial perturbation of wavenumber pair $(\bar{k}, m)$ normalized so that the energy at the initial time $\bar{t}_1$ is $J(\bar{t}_1) = 1$. At time $\bar{t}_q \equiv \alpha^{q-1} \bar{t}_1$ – or, equivalently, $t_q \equiv (q-1) \ln(\alpha)/\gamma$ – the energy of this disturbance is

$$J(\bar{t}_q) = \frac{J(\bar{t}_q)}{J(\bar{t}_{q-1})} \cdots \frac{J(\bar{t}_2)}{J(\bar{t}_1)}. \tag{2.14}$$

The gain $J(\bar{t}_{p+1})/J(\bar{t}_p)$ over the time interval $[\bar{t}_p, \bar{t}_{p+1}]$ with $1 \leqslant p \leqslant q-1$ can be expressed in terms of the non-dimensional quantities

$$\frac{J(\bar{t}_{p+1})}{J(\bar{t}_p)} = \frac{\int \left(\alpha \hat{u}(\alpha) \hat{u}^+(\alpha) + \alpha \hat{v}(\alpha) \hat{v}^+(\alpha) + \frac{1}{\alpha^2} \hat{w}(\alpha) \hat{w}^+(\alpha) \right) \hat{r} \, \mathrm{d}\hat{r}}{\int (\hat{u}(1) \hat{u}^+(1) + \hat{v}(1) \hat{v}^+(1) + \hat{w}(1) \hat{w}^+(1)) \hat{r} \, \mathrm{d}\hat{r}}, \tag{2.15}$$

where $\hat{u}(\alpha; \hat{k}_p, m)$, $\hat{v}(\alpha; \hat{k}_p, m)$, $\hat{w}(\alpha; \hat{k}_p, m)$ are obtained at time $\hat{t} = \alpha$ after integration of system (2.9) over the time period $[1, \alpha]$ for wavenumber pair $(\hat{k}_p, m)$ with $\hat{k}_p \equiv \bar{k} \delta_p$. The gain (2.15) can be bounded by the maximum energy amplification $\hat{G}(\hat{k}, m; \alpha, Re_\Gamma)$ that a disturbance of wavenumber pair $(\hat{k}, m)$ can achieve at time $\hat{t} = \alpha$.

After the above transformations and scalings we are now in a position to investigate the transient as well as the asymptotic evolution of perturbations evolving on

the Burgers vortex. To study the transient evolution of perturbations, one has to compute the maximum energy amplification $\max[I(\tau)/I(0)]$ reached at any given time $t=\tau$ (Schmid & Henningson (2001)). This can most easily be accomplished by working in the transformed time interval $[\bar{t}_1, \bar{t}_2]$ and computing $\hat{G}(\hat{k}, m; \alpha, Re_\Gamma)$ with $\alpha \equiv \exp(\gamma\tau)$. A complete study of this problem will be presented elsewhere. Instead, we will focus on the asymptotic stability of the steady Burgers vortex. We start by using the following inequality:

$$\frac{J(\bar{t}_{p+1})}{J(\bar{t}_p)} \leqslant \hat{G}(\hat{k}_p, m; \alpha, Re_\Gamma), \tag{2.16}$$

which, together with (2.14), yields an upper bound on $I(t_q)=J(\bar{t}_q)$ of the form

$$I(t_q) \leqslant \prod_{p=1}^{q-1} \hat{G}(\hat{k}_p, m; \alpha, Re_\Gamma) \quad \text{with} \quad \hat{k}_p = \left(\bar{k}\sqrt{\frac{\nu}{\gamma}}\right)\alpha^{(p-1)/2} \quad \text{and} \quad t_q \equiv (q-1)\frac{\ln\alpha}{\gamma}. \tag{2.17}$$

It is important to note that the non-dimensional axial wavenumber $\hat{k}_p = \bar{k}\sqrt{\nu/\gamma}\alpha^{(p-1)/2}$ increases with index p as we move from one sub-interval to the next, whereas the axial wavenumber $\bar{k}$ remains constant and the physical wawenumber $k(t)$ decreases with time. If, for a given azimuthal wavenumber m, there exists a critical wavenumber $\hat{k}_c$ beyond which the maximum gain $\hat{G}(\hat{k}, m; \alpha, Re_\Gamma)$ is strictly less than one, asymptotic stability of the Burgers vortex can be demonstrated as follows. First, the quantity $I(t_q)$ is bounded by expression (2.17). $I(t_q)$ tends to zero as the index q, and thus t_q, tends to infinity. This is a consequence of the fact that $I(t_1)$ is a product of gains $\hat{G}$ which, above a certain index p, become strictly smaller than one. Any perturbation evolving according to the linear operator of equation (2.4) must asymptotically behave in time as $t^n \exp(\sigma t)$; hence, the energy $I(t_q)$ must evolve as $t_q^{2n}\exp(2\sigma t_q)$. Since the quantity $I(t_q)$ tends to zero as time t_q goes to infinity, the exponential growth rate σ has to be either strictly negative or zero with $n<0$. Either condition then ensures the asymptotic stability of the Burgers vortex. We have therefore reduced the Burgers stability problem to computing the maximum energy gain $\hat{G}(\hat{k}, m; \alpha, Re_\Gamma)$ at time $\hat{t}=\alpha$. The presence of time-dependent coefficients in (2.9) prohibits the application of standard techniques of modal stability analysis. A more sophisticated method (for details of this procedure see Farrell & Ioannou 1996; Andersson, Berggren & Henningson 1999; Luchini 2000 or Schmid & Henningson 2001) computes the maximum energy gain $\hat{G}(\hat{k}, m; \alpha, Re_\Gamma)$ through an optimization problem that is best solved with the help of the equations adjoint to (2.9). A standard derivation of these equations yields

$$\frac{\hat{\mathrm{D}}\tilde{u}}{\hat{\mathrm{D}}\hat{t}} + \left(\frac{\partial \hat{V}^{2D}}{\partial \hat{r}} + \frac{\hat{V}^{2D}}{\hat{r}}\right)\tilde{v} = \frac{\partial \tilde{p}}{\partial \hat{r}} + \frac{1}{Re_\Gamma}\left[(\Delta^{2D}\tilde{\boldsymbol{u}})_{\hat{r}} + \frac{1}{\hat{t}^3}\frac{\partial^2 \tilde{u}}{\partial \hat{z}^2}\right], \tag{2.18a}$$

$$\frac{\hat{\mathrm{D}}\tilde{v}}{\hat{\mathrm{D}}\hat{t}} - 2\frac{\hat{V}^{2D}}{\hat{r}}\tilde{u} = \frac{1}{\hat{r}}\frac{\partial \tilde{p}}{\partial \theta} + \frac{1}{Re_\Gamma}\left[(\Delta^{2D}\tilde{\boldsymbol{u}})_{\theta} + \frac{1}{\hat{t}^3}\frac{\partial^2 \tilde{v}}{\partial \hat{z}^2}\right], \tag{2.18b}$$

$$\frac{\hat{\mathrm{D}}\tilde{w}}{\hat{\mathrm{D}}\hat{t}} = \frac{1}{\hat{t}^3}\frac{\partial \tilde{p}}{\partial \hat{z}} + \frac{1}{Re_\Gamma}\left[(\Delta^{2D}\tilde{\boldsymbol{u}})_{\hat{z}} + \frac{1}{\hat{t}^3}\frac{\partial^2 \tilde{w}}{\partial \hat{z}^2}\right], \tag{2.18c}$$

$$\frac{\partial \tilde{u}}{\partial \hat{r}} + \frac{\tilde{u}}{\hat{r}} + \frac{1}{\hat{r}}\frac{\partial \tilde{v}}{\partial \theta} + \frac{\partial \tilde{w}}{\partial \hat{z}} = 0, \tag{2.18d}$$

$$\frac{\hat{\mathrm{D}}}{\hat{\mathrm{D}}\hat{t}} \equiv -\frac{1}{Re_\Gamma}\frac{\partial}{\partial \hat{t}} - \frac{\hat{V}^{2\mathrm{D}}(\hat{r}, \hat{t})}{\hat{r}}\frac{\partial}{\partial \theta} \tag{2.18e}$$

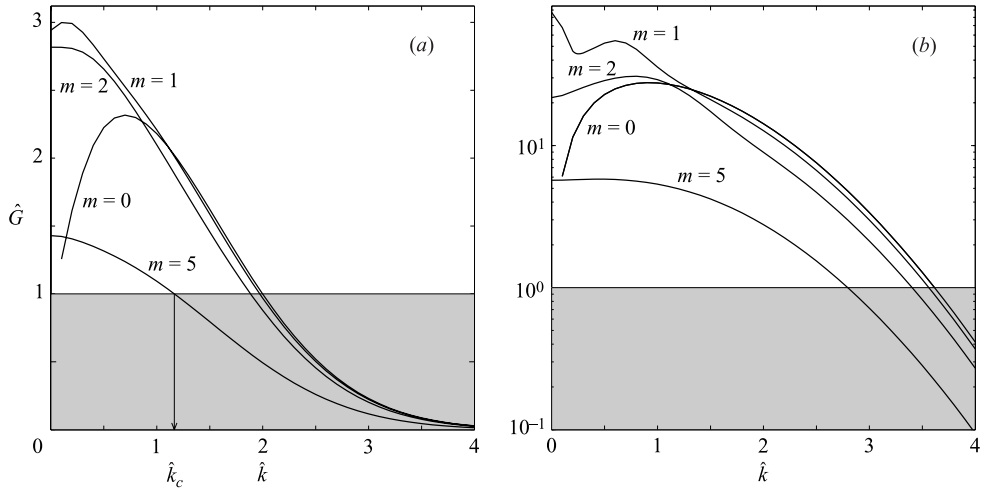

FIGURE 1. Maximum energy amplification $\hat{G}(\hat{k}, m; \alpha, Re_\Gamma)$ as a function of the axial wavenumber $\hat{k}$ and selected azimuthal wavenumbers m. Results for Reynolds numbers (*a*) $Re_\Gamma = 500$, (*b*) $Re_\Gamma = 5000$ are shown and $\alpha = 1.2$. Note the logarithmic scaling of the vertical axis in (*b*). In (*a*), the critical axial wavenumber is defined (for the case $m = 5$) as the axial wavenumber at which the energy amplification $\hat{G}$ drops below one (the shaded area).

with $\tilde{u}, \tilde{v}, \tilde{w}, \tilde{p}$ as the adjoint velocities and adjoint pressure. Since we only consider a specific wavenumber pair, the equations above are Fourier transformed along these coordinate directions. The adjoint equations (2.18) have to be solved backwards in time. An iterative scheme can then be devised which propagates a given initial condition forward in time using (2.9), the result of which serves as an 'initial' condition for the backward propagation by the adjoint equations (2.18). After one forward–backward integration an updated initial condition for the next iterative step is available. Convergence is reached when the initial condition for the forward problem does not change appreciably by an appropriately chosen criterion from one iterative step to the next. The maximum energy amplification can then be computed by propagating the converged initial condition forward in time and by forming the ratio of the disturbance energy at the end of the time interval to the energy at the beginning.

3. Results

The direct and adjoint equations, (2.9) and (2.18), respectively, have been discretized using a hybrid pseudospectral scheme based on rationally mapped Chebyshev polynomials. The number and distribution of collocation points has been adjusted to obtain grid-independent solutions.

The results of the iterative method to compute the maximum energy amplification $\hat{G}(\hat{k}, m; \alpha, Re_\Gamma)$ are displayed in figure 1 for two Reynolds numbers. We observe an energy amplification for small to moderate axial wavenumbers; for higher axial wavenumbers, however, the disturbance energy amplification is less than one and quickly approaches the asymptotic behaviour $\hat{G} \sim \exp(-\beta \hat{k}^2)$ with $\beta > 0$ as $\hat{k}$ tends to infinity. The critical axial wavenumber $\hat{k}_c$ above which the maximum

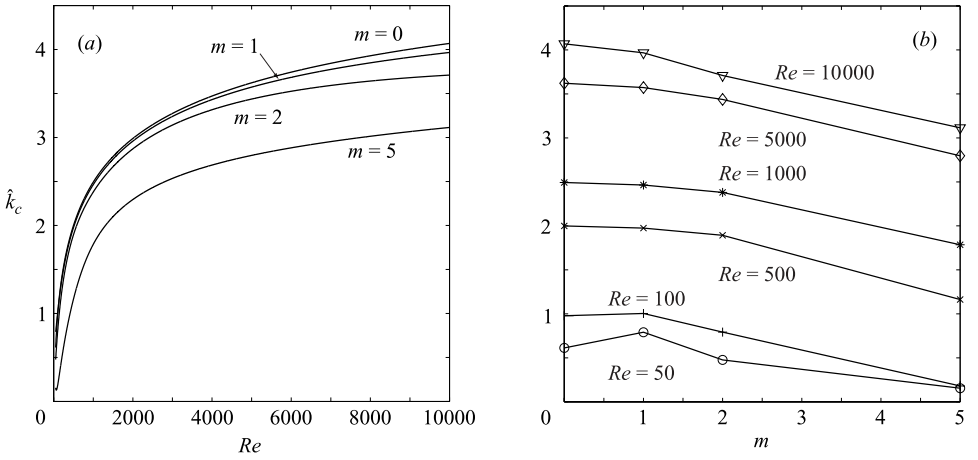

FIGURE 2. Critical axial wavenumber $\hat{k}_c$ as a function of (*a*) Reynolds number Re_Γ for $m = 0, 1, 2, 5$ and (*b*) azimuthal wavenumber m for $\alpha = 1.2$.

energy amplification $\hat{G}$ becomes less than one (see figure 1*a*), is computed and displayed in figure 2 as a function of the Reynolds number Re and the azimuthal wavenumber m. Critical wavenumbers are observed to decrease as m increases. In contrast, the critical wavenumbers increase with Reynolds number (but always exist). For higher Reynolds number, significant short-term amplification has been observed (note the logarithmic scaling on figure 1(*b*), i.e. for $Re_\Gamma = 5000$), but a comprehensive study of this phenomenon is left for a future effort. Finally, figure 3 illustrates the temporal evolution of the initial optimal condition corresponding to a maximum amplification at time $\bar{t} = \alpha \bar{t}_1$ (i.e. $t = \ln(\alpha)/\gamma$) for Reynolds number $Re_\Gamma = 1000$, axial wavenumber $\bar{k} = 0.5$, i.e. $\bar{k}(0) = 0.5/\delta_1$, and azimuthal wavenumber m (three wavenumbers have been selected $m = 1, 2, 5$). Times $\bar{t} = \alpha \bar{t}_1, \alpha^2 \bar{t}_1, \alpha^3 \bar{t}_1, \alpha^4 \bar{t}_1$, i.e. $t = \ln(\alpha)/\gamma, 2\ln(\alpha)/\gamma, 3\ln(\alpha)/\gamma, 4\ln(\alpha)/r$, with $\alpha = 1.2$ are shown. We observe in all three cases that the mechanism of energy amplification appears to be associated with a relaxation of the initial disturbance (at $\bar{t} = \bar{t}_1$) opposing the mean swirl, followed by an azimuthal roll-up of the axial perturbation vorticity.

4. Summary and conclusions

The stability of a Burgers vortex with respect to three-dimensional perturbations has been considered. An extended Lundgren transformation, together with a disection of the time axis and an appropriate nondimensionalization, reduced the full stability problem to a system of equations that describes the evolution of perturbations over a finite time period based on a time-dependent simplified mean flow. Using the adjoint stability equations, bounds on the maximum attainable growth of disturbance energy have been computed. These bounds show that the Burgers vortex is *asymptotically stable* to three-dimensional disturbances of infinitesimal amplitudes.

P. J. S. would like to thank the Université Pierre et Marie Curie for its support and warm hospitality during his stay as *enseignant invité*. We are also indebted to Olivier Daube (LIMSI) for his assistance in the early stage of this work.

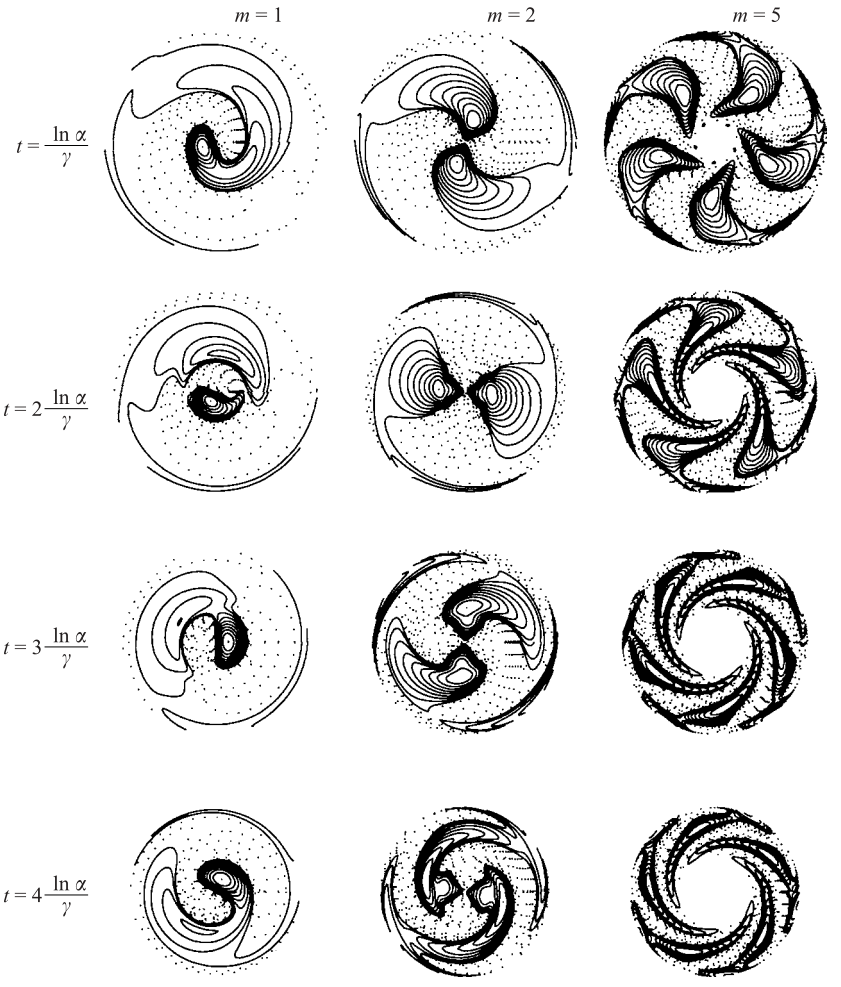

FIGURE 3. Temporal evolution of the axial component of the vorticity perturbation ω_z shown as isocontours in the (r, θ)-plane at a fixed axial location and for selected azimuthal wavenumbers m. See the text for the chosen initial conditions. At each time t, twenty contours levels are plotted $\pm(i/10)^2\omega_{z,\max}(t)$ with $i = 1, 2, \ldots, 10$. Positive (negative) contour levels are represented by solid (dotted) lines. Snapshots were taken at $t = \ln(\alpha)/r, 2\ln(\alpha)/\gamma, 3\ln(\alpha)/\gamma, 4\ln(\alpha)/\gamma$, with $\alpha = 1.2$ and cut in the radial direction at $\bar{r} = 10\,a_0$ where a_0 is the Burgers vortex size. The Reynolds number is $Re_\Gamma = 1000$; the initial axial wavenumber $k(t=0)$ is such that $k(t=0) = \bar{k} = 0.5/\delta_1$.

REFERENCES

ANDERSSON, P., BERGGREN, M. & HENNINGSON, D. S. 1999 Optimal disturbances and bypass transition in boundary layers. *Phys. Fluids* **11**, 134–150.

BATCHELOR, G. K. & PROUDMAN, I. 1954 The effect of rapid distortion on a fluid in turbulent motion. *Q. J. Mech. Appl. Math.* **7**, 83–103.

CADOT, O., DOUADY, S. & COUDER, Y. 1995 Characterization of the low pressure filaments in three-dimensional turbulent shear flow. *Phys. Fluids* **7**, 630–646.

CAMBON, C. & SCOTT, J. F. 1999 Linear and nonlinear models of anisotropic turbulence. *Annu. Rev. Fluid Mech.* **31**, 1–53.

CRAIK, A. D. D. & CRIMINALE, W. O. 1986 Evolution of wavelike disturbances in shear flows: a class of exact solutions of the Navier-Stokes equations. *Proc. Roy. Soc. Lond.* A **406**, 13–26.

Crowdy, D. G. 1998 A note on the linear stability of Burgers vortex. *Stud. Appl. Maths.* **100**, 107–126.

Eloy, C. & Le Dizès, S. 1999 Three-dimensional instability of Burgers and Lamb–Oseen vortices in a strain field. *J. Fluid Mech.* **378**, 145–166.

Farrell, B. F. & Ioannou, P. J. 1996 Generalized stability theory. Part I: Autonomous operators. Part II: Nonautonomous operators. *J. Atmos. Sci.* **53**, 2025–2053.

Gibbon, J. D., Fokas, A. S. & Doering, C. R. 1999 Dynamically stretched vortices as solution of the 3D Navier–Stokes equations. *Physica* D **132**, 497–510.

Jiménez, J., Wray, A. A., Saffman, P. G. & Rogallo, R. S. 1993 The structure of intense vorticity in isotropic turbulence. *J. Fluid Mech.* **255**, 65–90.

Le Dizès, S., Rossi, M. & Moffatt, H. K. 1996 On the three-dimensional instability of an elliptical vortex subjected to stretching. *Phys. Fluids* **8**, 2084–2090.

Leibovitch, S. & Holmes, P. 1981 Global stability of the Burgers' vortex. *Phys. Fluids* **24**, 548–549.

Luchini, P. 2000 Reynolds number independent instability of the boundary layer over a flat surface: optimal perturbations. *J. Fluid Mech.* **404**, 289–309.

Lundgren, T. S. 1982 Strained spiral vortex model for turbulent fine structure. *Phys. Fluids* **25**, 2193–2203.

Moffatt, H. K., Kida, S. & Ohkitani, K. 1994 Stretched vortices — the sinews of turbulence; large-Reynolds-number asymptotics. *J. Fluid Mech.* **259**, 241–264.

Prochazka, A. & Pullin, D. I. 1995 On the two-dimensional stability of the axisymmetric Burgers vortex. *Phys. Fluids* **7**, 1788–1790.

Pullin, D. I. & Saffman, P. G. 1998 Vortex dynamics in turbulence. *Annu. Rev. Fluid Mech.* **30**, 31–51.

Robinson, A. C. & Saffman, P. G. 1984 Stability and structure of stretched vortices. *Stud. Appl. Maths.* **70**, 163–181.

Rossi, M. 2000 Of vortices and vortical layers: an overview. In *Vortex Structure and Dynamics.* Lecture notes in Physics (ed. A. Maurel & P. Petitjeans) pp 40–123. Springer.

Rossi, M. & Le Dizès, S. 1997 Three-dimensional stability spectrum of stretched vortices. *Phys. Rev. Lett.* **78**, 2567–2569.

Saffman, P. G. 1992 *Vortex Dynamics.* Cambridge University Press.

Schmid, P. J. & Henningson, D. S. 2001 *Stability and Transition in Shear Flows.* Applied Mathematical Sciences, vol. 142, Springer.

Verzicco, R., Jiménez, J. & Orlandi, P. 1995 On steady columnar vortices under local compression. *J. Fluid Mech.* **299**, 367–388.

Vincent, A. & Meneguzzi, M. 1991 The spatial structure and statistical properties of homogeneous turbulence. *J. Fluid Mech.* **225**, 1–20.